Pest disintegration of thin $MoSi_2$ films by oxidation at 500 °C

T. C. CHOU*
Lockheed Research and Development Division, 3251 Hanover St., Palo Alto, CA 9430, USA
T. G. NIEH
Lawrence Livermore National Laboratory, P.O. Box 808, L-350, Livermore, CA 94550, USA

Thin molybdenum disilicide ($MoSi_2$) films have been produced by magnetron sputter deposition, and subjected to oxidation tests for the study of "$MoSi_2$ pest" – a phenomenon showing disintegration of a solid piece of $MoSi_2$ into powdery products. The as-prepared films were of an amorphous structure. Oxidation of the films in air at 500 °C led first to cracking of the films, and then the cracked pieces eventually evolved into disintegrated powders with a yellowish appearance. Secondary electron microscopy and Auger electron spectroscopy revealed that the reaction products consisted of MoO_3 whiskers (platelets), Si–Mo–O fibres, SiO_2 clusters, and some residual $MoSi_2$. The disintegration of $MoSi_2$ films appeared to be independent of their crystal structure; a similar phenomenon was also observed in crystallized films, with a metastable hexagonal structure, oxidized under the same conditions. The disintegration of the $MoSi_2$ films is compared to and correlated with the "pest reaction" of bulk $MoSi_2$.

1. Introduction

Molybdenum disilicide ($MoSi_2$) is a well-known high melting point intermetallic compound. Being a metal-like thermally stable conductor with exceptional oxidation resistance up to 1900 °C in air, $MoSi_2$ has found many applications, such as electrical heating elements in high-temperature furnaces, protective coatings for high-temperature structural materials [1–4], and electrical contacts and/or interconnects in silicon device technology [5–8]. Because of its technological importance as an engineering material for both structural and electronic applications, extensive research efforts have been spent on the material synthesis, characterization, and mechanical properties of both bulk and thin films of $MoSi_2$.

In spite of its superior environmental protective capabilities at high temperatures, $MoSi_2$ suffers from the so-called "pest reaction" during low-temperature (400–600 °C) oxidation [1, 9–11]. The pest of $MoSi_2$ is characterized by the total disintegration of the sample into powdery products. Although pest was first discovered by Fitzer in 1955 [1], the fundamental understanding of its origin is not yet established. Based on some very recent studies from the low-temperature oxidation of $MoSi_2$, pest occurs not only in hot-pressed and cast polycrystalline materials [12, 13], but also in single-crystalline $MoSi_2$ bulk samples [13]. As a result, powdery products were formed and they contained MoO_3 whiskers, SiO_2 clusters, and some residual $MoSi_2$ crystals. Moreover, the results from the study of single crystals indicated that pest reaction was a nucleation-controlled kinetic process. The nuclei were present in the form of blisters, caused by the combined effects of thermal mismatch between Si–Mo–O surface oxide and $MoSi_2$ substrate, and internal vapour pressures resulting from the formation of volatile MoO_3 [13]. A detailed mechanism for $MoSi_2$ pest will be presented elsewhere [14].

Although pest reactions have been observed in $MoSi_2$ bulk samples, experimental results on the pest of $MoSi_2$ films have not been reported to date. It is worth noting that a few other refractory-metal disilicides (e.g. WSi_2, $FeSi_2$, $NbSi_2$, and $MnSi_2$) that have been extensively used for the oxidation protection of high-temperature structural materials, are also reported to exhibit pest disintegration at various temperature regimes [15]. Not all these refractory-metal disilicides, when present as a coating film, however, have been observed to be susceptible to pest reactions [16–18]. In this letter, we record the first finding of pest reaction in monolithic $MoSi_2$ films.

2. Experimental procedure

The $MoSi_2$ films were deposited by d.c. magnetron sputtering from a hot-pressed $MoSi_2$ target (20 cm diameter and 6.5 mm thick, purchased from Cerac Inc.) on Si (1 1 1) substrates. The composition and structure of the target were examined by Auger electron spectroscopy (AES) and X-ray diffraction (XRD), and confirmed to be $MoSi_2$ with a tetragonal crystal structure. In addition, scanning electron microscopy (SEM) and energy dispersive spectrometry X-ray microanalysis (EDS) indicated that the hot-pressed

* Present address: The BOC Group Technical Center, 100 Mountain Avenue, Murray Hill, NJ 07974, USA

0022–2461 © *1994 Chapman & Hall*

$MoSi_2$ contained a small amount of SiO_2 and Mo_5Si_3 (in the vicinity of the SiO_2) as a result of oxidation during sample preparation.

Prior to deposition, the base pressure was about 1×10^{-5} Pa. During the sputter deposition of $MoSi_2$, the substrates were first sputter cleaned under 200 V, d.c. reverse bias, and 0.67 Pa argon gas pressure for 4 min. Typical deposition parameters used in this study were 1 kW power and 0.67 Pa processing gas (argon) pressure. The deposition rate under such conditions was calibrated to be about 10.5 nm min^{-1}. The typical thickness of the $MoSi_2$ films made for this study was 1.2 μm. The composition of the resulting films was then analysed by AES, and the structure was examined by transmission electron microscopy (TEM). It is pointed out that no substrate heating was applied during sample preparation and the overall temperature of the films during deposition, monitored by using heat-sensitive tapes, was found to be no more than 80 °C.

The films were then oxidized in air (relative humidity 55%, water vapour pressure ~ 1740 Pa) at 500 °C for different periods of time. The morphologies of the films were examined using optical microscopy and scanning electron microscopy (SEM). Composition of the reaction products after oxidation was investigated by AES. (Typical electron-beam size used for AES analysis was about 150 nm.) The structures of the reaction products were examined by XRD and a Jeol 2000FX TEM.

3. Results and discussion

An AES depth concentration profile from an as-deposited $MoSi_2$ film (100 nm thick) is given in Fig. 1. It is noted that the atomic ratio between molybdenum and silicon is about 1:2 and remains to be constant throughout the film. The amounts of carbon and oxygen (contaminants) present in the film are negligible. This concentration profile is similar to that obtained from the hot-pressed $MoSi_2$ standard.

Transmission electron microscopy (TEM) bright-field images and electron diffraction patterns revealed that the as-prepared film was in an amorphous state, although a few crystallites with lateral dimensions of a few nanometres are occasionally observed near the edge of the films. The interatomic spacings of those crystallized regions, however, cannot be resolved clearly by high-resolution TEM. A detailed study on the microstructural evolution (as a function of temperature) and mechanical properties of the $MoSi_2$ films can be found elsewhere [19].

After oxidation at 500 °C for only a short period of time, severe cracking and delamination were observed on the films. Fig. 2a presents a scanning electron micrograph showing the morphological features of a film after oxidation for 5 min. It is interesting to note in Fig. 2a that some of the delamination occurs within the silicon substrate (manifested by the presence of cleavage striations as indicated by arrows), rather than at the film/substrate interface, suggesting a relatively strong bonding between the $MoSi_2$ film and the silicon substrate in some local regions. Upon prolonged oxidation, the cracked $MoSi_2$ films transformed into powders with a yellowish appearance. A scanning electron micrograph showing the morphological characteristics of the film after oxidation for 24 h is

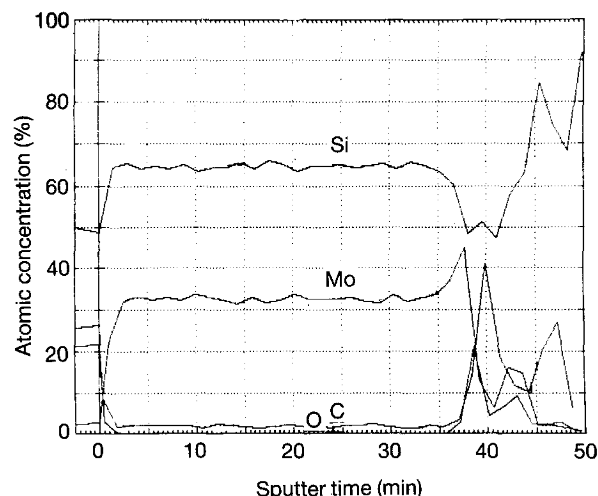

Figure 1 AES depth concentration profiles of an as-deposited $MoSi_2$ film.

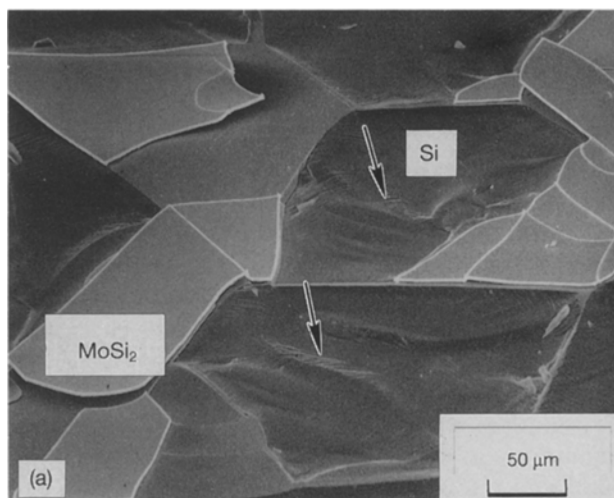

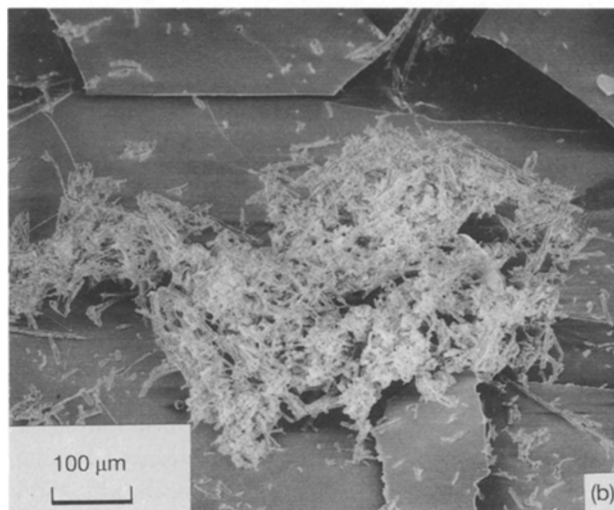

Figure 2 Scanning electron micrographs showing the morphologies of $MoSi_2$ films (a) after oxidation at 500 °C for 5 min, and (b) after prolonged oxidation at 500 °C for 24 h.

presented in Fig. 2b. Most of the cracked $MoSi_2$ pieces convert to agglomerated, feather-like powders.

The detailed morphological features of the powders are delineated in Fig. 3. The morphologies of the reaction products can be categorized into needle (platelet), cluster, and some residual $MoSi_2$ pieces. Most of the needle-like reaction products show irregular surface features (denoted fibres hereafter), although some of them exhibit smooth and regular geometry (denoted whiskers hereafter). According to AES analyses, the whiskers are predominantly MoO_x (Fig. 4a) and the fibres contain silicon, molybdenum and oxygen (Fig. 4b), while the clusters were mainly SiO_2. Using the sensitivity factors of 0.73 and 0.43 (based on an MoO_3 standard) for molybdenum and oxygen, respectively, the MoO_x was determined to be MoO_3. It is noted that the amount of molybdenum present in the Si–Mo–O fibres varies significantly, suggesting that either the composition of these fibres is not in an equilibrium state or they contain a mixture of SiO_2 and MoO_3 phases. However, based upon the previous study of oxidation of $MoSi_2$ single crystals [13], Si–Mo–O may be present as a transient oxide, which would evolve into MoO_3 whiskers and SiO_2 clusters upon further oxidation.

The reaction products found in the present study are very similar to those observed in the disintegrated $MoSi_2$ bulk samples, which were also subjected to oxidation at 500 °C. Fig. 5a and b, respectively, show an optical micrograph of a disintegrated, hot-pressed $MoSi_2$ bulk sample after oxidation in air for 21 h, and a scanning electron micrograph showing the morphological details of the powders. According to the AES, XRD, and TEM analyses, the powdery products consisted of MoO_3 whiskers (needles/platelets), SiO_2 clusters, and some residual $MoSi_2$ crystals. Transmission electron micrographs and the corresponding electron diffraction patterns indicated that the MoO_3 whiskers had an orthorhombic crystal structure (see Fig. 6a and b), while the SiO_2 clusters were mainly amorphous (see Fig. 7a and b). The longitudinal axes of the MoO_3 whiskers were found to be parallel to the a-axis of the orthorhombic unit cell ($a = 0.396$ nm, $b = 1.386$ nm, $c = 0.370$ nm).

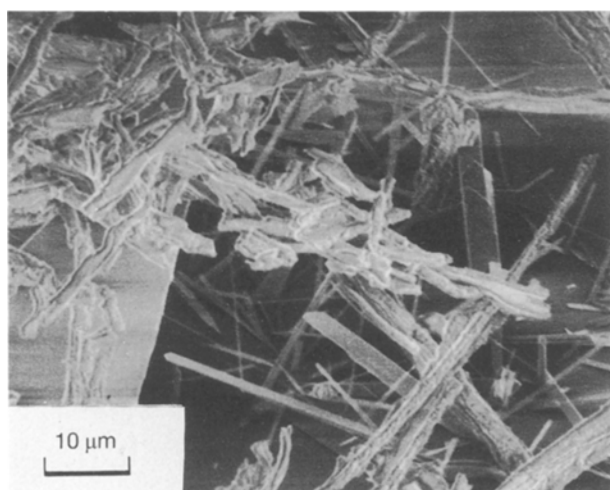

Figure 3 Scanning electron micrograph showing the typical morphologies of the reaction products observed in the disintegrated $MoSi_2$ film.

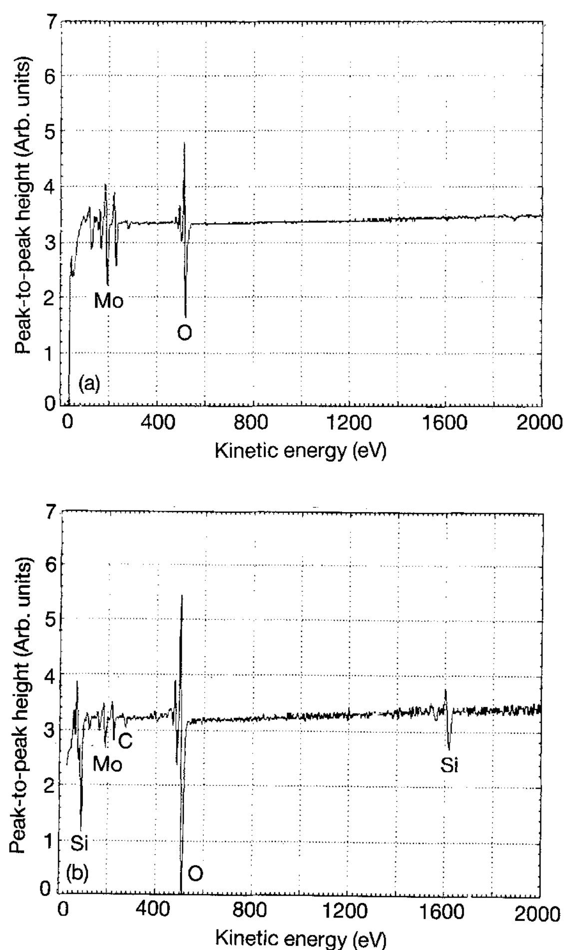

Figure 4 AES spectra of (a) a MoO_3 whisker and (b) a Si–Mo–O fibre from the disintegrated powders.

It is evident that thin $MoSi_2$ films behave similarly to bulk $MoSi_2$ during low-temperature oxidation – both materials are susceptible to pest reactions, and they disintegrated into powders of MoO_3 whiskers, SiO_2 clusters, and some residual $MoSi_2$. Because the as-prepared $MoSi_2$ films were of an amorphous structure, a question yet to be answered is whether or not the observed pest reaction is dependent upon the structure of the films. Molybdenum disilicide is known to exist in two different crystal structures – a metastable, hexagonal structure and the thermodynamically stable, tetragonal structure [20]. In the present study of $MoSi_2$ pest by oxidation, monitoring the structural evolution of the films prior to pest reaction is considered to be difficult. As a result, the amorphous films were crystallized initially at 300 °C (into a hexagonal structure) [19] and, then, oxidized at 500 °C. It was found that the crystallized films also underwent pest reaction, and disintegrated into powdery products of MoO_3 whiskers, Si–Mo–O fibres, SiO_2 clusters, and some unreacted $MoSi_2$. Fig. 8 presents a scanning electron micrograph showing the typical characteristics of the reaction products.

As far as crystallizing the films into a tetragonal structure is concerned, previous study indicated that

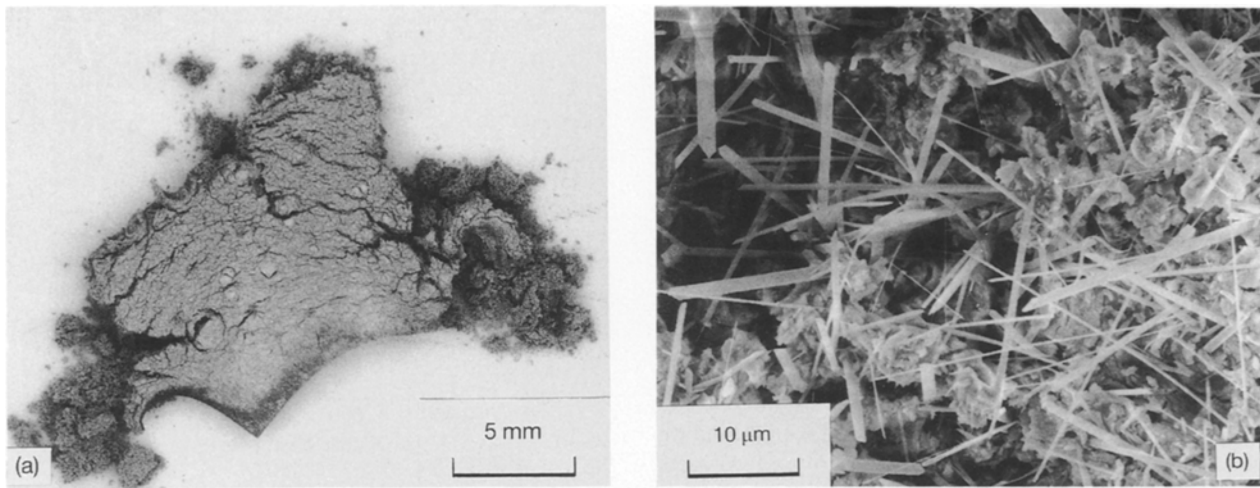

Figure 5 (a) An optical micrograph showing the characteristics of a disintegrated, hot-pressed polycrystalline $MoSi_2$ bulk. (b) A scanning electron micrograph showing the typical morphologies of the reaction products in the powders.

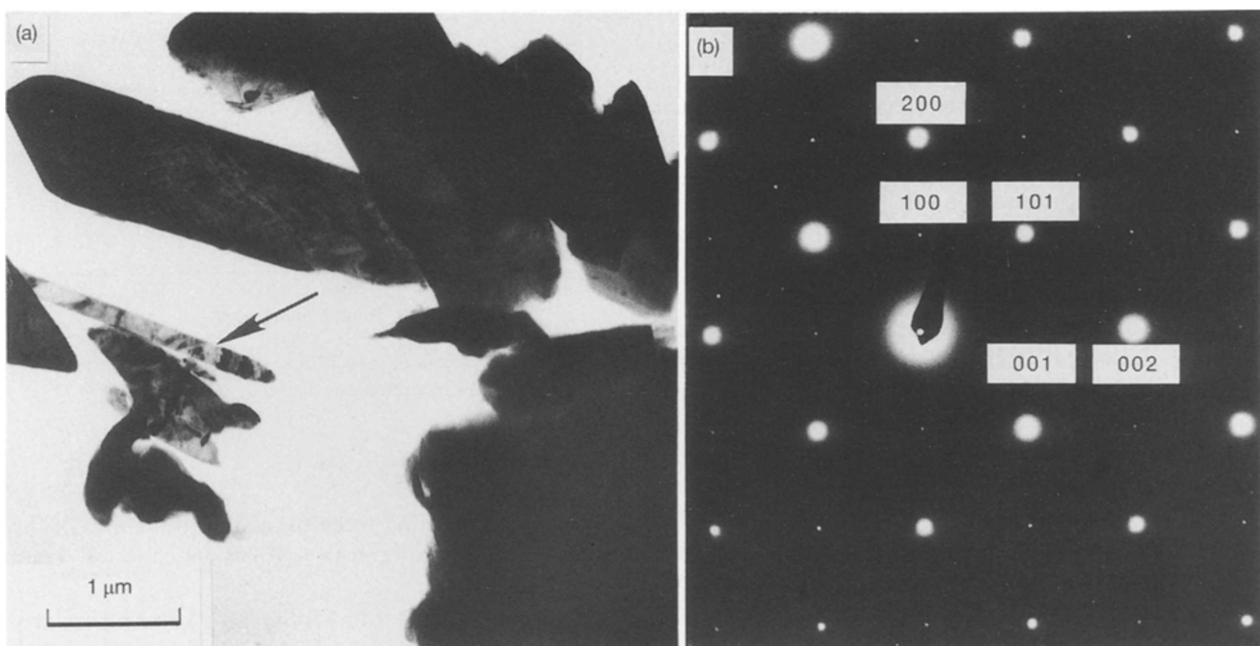

Figure 6 (a) A transmission electron micrograph and (b) the corresponding electron diffraction pattern of a MoO_3 whisker, as indicated by an arrow in (a).

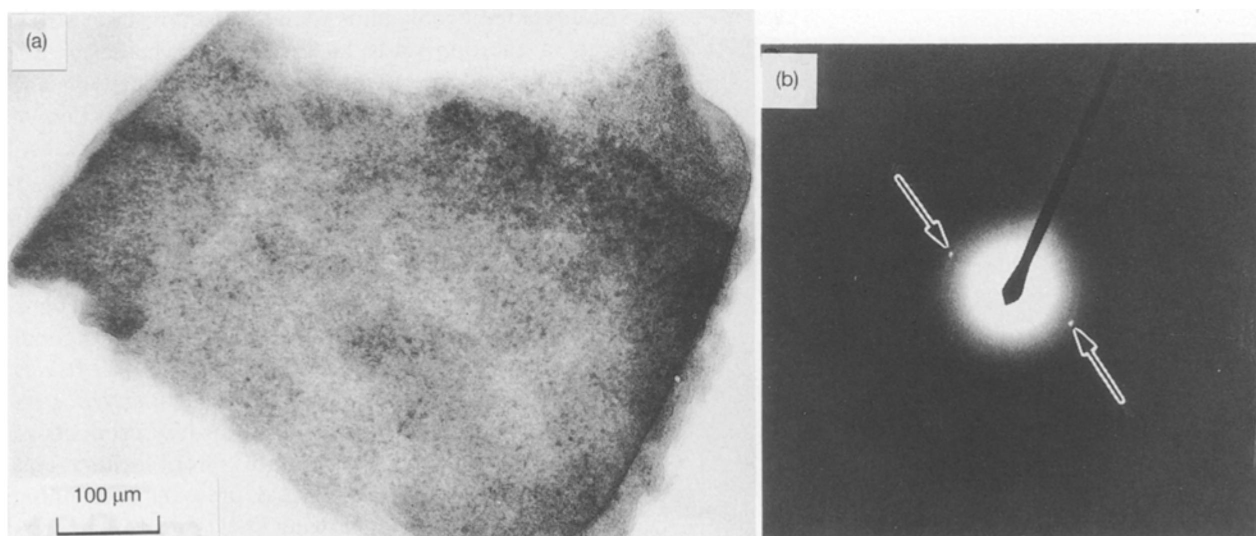

Figure 7 (a) A transmission electron micrograph and (b) the corresponding electron diffraction pattern of an SiO_2 cluster. The discrete spots, indicated by arrows in (b), have a *d*-spacing of 0.39 nm, which is attributable to the presence of {0 0 2} residual, tetragonal-$MoSi_2$.

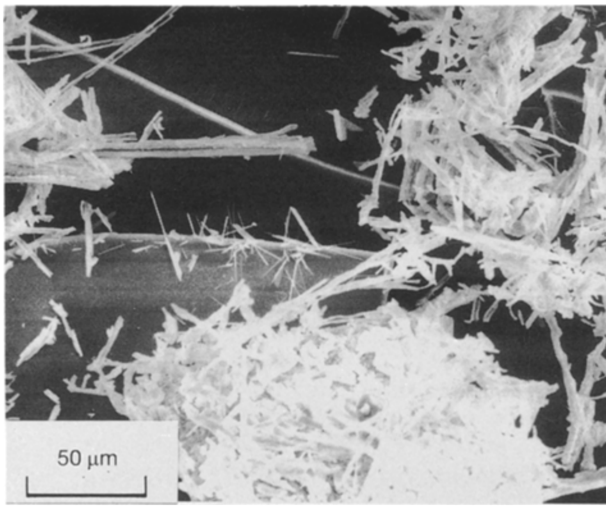

Figure 8 A scanning electron micrograph showing the morphological features of the powdery products from a pre-crystallized $MoSi_2$ film after oxidation at 500 °C for 17 h.

the structural transformation from hexagonal to tetragonal took place only at temperatures above 800 °C [19]. Moreover, the phase transformation process was accompanied with the formation of tetragonal Mo_5Si_3; the films contained a mixture of tetragonal $MoSi_2$ and tetragonal Mo_5Si_3. Although it is yet to be confirmed, $MoSi_2$ films with a tetragonal structure are believed also susceptible to pest reaction. This is based on the fact that both hot-pressed and cast polycrystalline $MoSi_2$ (tetragonal structure) show pest reaction at 500 °C.

In summary, magnetron sputter-deposited $MoSi_2$ films of both amorphous and hexagonal structures were found to be susceptible to "pest reaction" at 500 °C in air. The pested films disintegrated into agglomerated, powdery products. The reaction products formed were characterized to consist of MoO_3 whiskers, Si–Mo–O fibres, SiO_2 clusters, and some residual $MoSi_2$; these are similar to those observed in bulk $MoSi_2$ after pest. Experimental results also indicated that the crystallographic structures had little effect on the pest reaction of $MoSi_2$.

Acknowledgements
The authors thank Dr H. S. Hu for the AES analysis. This work was supported by the Naval Air Development Center under contract N62269-89-0261, monitored by Dr G. J. London.

References
1. VON E. FITZER, in "Plansee Proceedings, 2nd Seminar" (Reutte/Tyrol, 1956) pp. 56–79.
2. C. D. WIRKUS and D. R. WILDER, *J. Am. Ceram. Soc.* **49** (1966) 173.
3. H. H. HAUSNER (ed.), "Coatings of High Temperature Materials" (Plenum, New York, 1966).
4. G. V. SAMSONOV, "Silicides and Their Uses in Engineering" (Akad. Nauk. Ukr. SSR, Kiev, 1959).
5. A. GUIVARC'H, P. AUVRAY, L. LE CUN, J. P. BOULET, G. PELOUS and A. MARTINEZ, *J. Appl. Phys.* **49** (1978) 233.
6. A. PERIO, J. TORRES, G. BOMCHIL, F. ARNAUD D'AVITAYA and R. PANTEL, *Appl. Phys. Lett.* **45** (1984) 857.
7. S. P. MURARKA, "Silicides for VLSI Applications" (Academic Press, New York, 1983).
8. F. M. D'HEURLE, C. S. PETERSSON and M. Y. TSAI, *J. Appl. Phys.* **51** (1980) 5976.
9. J. J. RAUSCH, ARF 2981-4, Armour Research Foundation, 31 August 1961, NSA 15-31171.
10. E. A. AITKEN, in "Intermetallic Compounds", edited by J. H. Westbrook (Wiley, New York, 1967) pp. 491–516.
11. P. J. MESCHTER, *Met. Trans.* **23A** (1992) 1763.
12. T. C. CHOU and T. G. NIEH, *Scripta Metall. Mater.* **26** (1992) 1637.
13. *Idem, ibid.* **27** (1992) 19.
14. *Idem, J. Mater. Res.* **8** (1993) 214.
15. J. H. WESTBROOK and D. L. WOOD, *J. Nucl. Mater.* **12** (1964) 208.
16. C. H. HO, S. PRAKASH, H. J. DOERR, C. V. DESHPANDEY and R. F. BUNSHAH, *Thin Solid Films* **207** (1992) 294.
17. A. L. PRANATIS, C. I. WHITMAN and C. D. DICKINSON, "Summary of the 5th Meeting of the Refractory Composites Working Group", Defense Metals Information Center Report 167, March 1962.
18. R. A. PERKINS, private communication (1992).
19. T. C. CHOU and T. G. NIEH, *Thin Solid Films* **214** (1992) 48.
20. A. B. GOKHALE and G. J. ABBAASCHIAN, in "Binary Alloy Phase Diagrams", Vol. 1, edited by T. B. Massalski, J. L. Murray, L. H. Bennett and H. Baker (ASM, Metals Park, OH, 1986) p. 1632.

Received 6 April
and accepted 16 June 1993